EFFECT OF MEGA-CONSTELLATIONS ON COLLISION RISK IN SPACE

C. Álvaro Arroyo-Parejo, Noelia Sánchez-Ortiz, and Raúl Domínguez-González

DEIMOS Space S.L.U., Ronda de Poniente 19, Tres Cantos, Madrid, 28760 Spain, Email: {carlos.arroyo, noelia.sanchez, raul.dominguez}@deimos-space.com

ABSTRACT

The number of companies aiming to launch mega constellations into space is increasing. The majority of them are supposed to be deployed in Low Earth Orbit (LEO) regions where the population of space debris is most concentrated. This change in the industry requires developments in collision risk analysis since, in case of satellite failure, the probability that one of them collides with a piece of space debris is not negligible, and the satellite would potentially break apart creating more space debris. Therefore, a collision would ultimately increase the overall collision risk, leading to the well-known Kessler syndrome.

This paper discusses the investigation of how mega-constellations will affect the space environment in terms of collision risk. At first, an overview of the different mega-constellations has been carried out in order to provide orbit definition and orbital lifetime for different scenarios. Then, different methods and mathematical tools to compute the collision risk have been considered. ESA-MASTER has been used to compute the flux during the complete orbital lifetime with the purpose of estimating the mean number of collisions and the impact probability for the entire constellation. Since these constellations are formed by hundreds or thousands of satellites, the endogenous and exogenous encounters have been also computed for objects in a mega-constellation. Thus, the impact of a collision cloud on the constellation has been characterised. This analysis has been made following two different approaches: the collision of a single object of the constellation with an external space debris, and the failure of a satellite of the constellation which leads to a collision with a second constellation object. The study has determined the impact on the space debris environment and the flux evolution after the encounter. Due to the number of objects, the constellation and the catalogue, it is necessary to optimise the evaluation of the encounters with the aim of reducing the computational expense of the implementation.

Keywords: *mega-constellations; flux analysis; collision probability, space debris*.

1. INTRODUCTION

During the last decade, the space sector has been witnessing a change in trend, giving way to what is currently known as "New Space". This change in trend has led, among other things, to the miniaturisation of satellites (nanosatellites, picosatellites, etc,) and their mass production by private companies. According to the latest ESA's environmental space report [1], the number of objects in the low Earth orbit (LEO) regions continues to increase, this being the orbital regime with the largest number of active objects. In addition, the largest number of objects in this regime corresponds, nowadays, to commercial missions. It is in this context that the emergence of commercial proposals related to worldwide broadband constellations projects becomes important, as they threaten the future sustainability of space and space operations. These mega-constellation plans, from private companies (Starlink, OneWeb, Amazon Kuiper, etc.), consist of thousands of satellites located at LEO or very low Earth orbit (VLEO) regimes in which, as aforementioned, the majority of current operational satellites and space debris objects reside. The main problem lies within the fact that, if all these projects were to come to fruition, the number of tracked objects currently in space could triple in a few years. Increasing the number of objects raises the collision risk. The risk of causing a chain reaction due to the collision between space debris objects (the well-known Kessler syndrome [2]) has been analysed in numerous studies [3, 4, 5, 6, 7], concluding that in the event of such collisions, the LEO regime could become inaccessible or accessible at high risk, and remain so for hundreds of years, endangering future manned flights. Owing to the aforementioned reasons, several recent studies have tried to highlight how the risk of collision would be greatly affected by the appearance of these mega-constellations. Some of these studies have tried to analyse the mean number of collisions and the probability of collision for a constellation object and for the whole constellation [8, 9, 10]. Moreover, these analysis include each and every stage of the constellation: ascent, nominal orbit and disposal. Alongside these, the impact on the number of collision avoidance manoeuvres that would have to be performed [9, 10], and on how different post-mission disposal (PMD) strategies would affect to reduce collision probability [11] has been analysed. Both higher satellite mass and constellation orbit altitude are also an important factor in terms of Collision

Proc. 8th European Conference on Space Debris (virtual), Darmstadt, Germany, 20–23 April 2021, published by the ESA Space Debris Office
Ed. T. Flohrer, S. Lemmens & F. Schmitz, (http://conference.sdo.esoc.esa.int, May 2021)

rate percentage increase (CRI) [12]. In spite of these researches, it is certain that these mega-constellations will be operative in the coming years. Consequently, other studies have tried to evaluate how this collision risk will affect the design of future mega-constellations [13] or assess and propose ways to mitigate possible collisions that may occur [14].

Another problem encountered when analysing these mega-constellations is the opacity and lack of information in some of their data (e.g., the geometry and size of the satellites or the the characteristics of the propulsion subsystem). Subsequently, some of the parameters used during this and other studies make some assumptions to characterize the problem. Fortunately, the characteristics of the orbits used in the OneWeb and Starlink constellations analysed in this study have been published through the Federal Communications Commission (FCC) [15, 16, 17] (as for the Amazon Kuiper project [18]). In addition, this analysis assumes that both projects take into consideration the international debris mitigation guidelines proposed by the United Nation's Committee on the Peaceful Uses of Outer Space (UNCOPUOS). In this paper, the collision probability risks analysed correspond to the OneWeb and Starlink projects for two main reasons: they are the two projects that are currently being launched, and thereafter, the information on them is more accessible and has been gathered in other analyses. It is important to underline that most of the analyses performed in this study have been carried out using public access software tools (DRAMA software tools suite, MASTER-2009 and MASTER-8) which are provided by the European Space Agency through the Space Debris User Portal (SDUP).

The structure of this document is as follows. Section 2 summarizes the characteristics of the orbits used, as well as the geometry of the satellites that form the mega-constellations. The methodology applied in this analysis is described in Section 3. The results of the flux, mean number of collisions, probability of collision, and the impact of collision clouds are discussed in Section 4. Finally, Section 5 presents the main conclusions drawn from this study and possible future work.

2. MAIN PARAMETERS OF MEGA-CONSTELLATIONS

The Starlink (SpaceX), OneWeb (OneWeb and Airbus), and Kuiper (Amazon) mega-constellations are the three major projects proposed to provide high-speed broadband and global Internet coverage. They are classified as Non-geostationary satellite orbit systems (NGSO) [9]. Currently, only the satellites of the first two constellations are being launched, and there is no information regarding the satellites of the Amazon Kuiper one, so the analysis will focus on Starlink and OneWeb. Both proposals are expected to launch thousands of satellites that will be located in Low Earth Orbit or Very Low Earth Orbit, for Starlink second generation. The information regarding the configuration of the different orbits of both constellations has been compiled since publication of the technical details issued by each of the companies to the FCC [15, 16, 18]. These initial proposals placed the OneWeb constellation at an altitude of 1200 km while the Starlink constellation consisted of orbits located at different altitudes: 550, 1110, 1130, 1275 and 1325 km. In addition, the proposed modification of Starlink for its first generation has also been considered in the analysis [17]. In this proposal, altitudes higher than 1000 km have been reduced to altitudes between 540 and 570 km. Also, OneWeb's second generation proposal to increase the number of satellites to around 48000 for the same altitude will be taken into account (although the company has recently stated that the number of satellites will be drastically reduced to about 6372). Furthermore, the following assumptions have been made for both constellations:

- The operational phase lifetime of each satellite within the constellation will be 5 years.
- The operational lifetime of the total constellation will be 10 years.
- The spacecraft failure rate will vary between 2.5% and 5%.

According to the latest *ESA's Annual Space Environment Report* [1], the population of objects in LEO is larger between 300 km and 800 km, where the Starlink modification would be located. It must also be taken into account that both the OneWeb constellation and the first Starlink proposal are located at altitudes above 800 km, and therefore, both their ascent and disposal will pass through those altitudes increasing the flux and, thus, the probability of collision. However, this probability of collision will be lower than that of the nominal orbit because the duration with respect to it is also shorter. In addition, most of the tracked objects in these orbits correspond to space debris which increase the indeterminacy of the objects' orbits. This is because, currently, the catalogue of tracked objects consists of those objects with diameters greater than 10 cm [19] obtained through direct observations; while diameters smaller than 10 cm, the catalogue of objects is based on indirect observations and mathematical models, which generates a large uncertainty in the measurements [20].

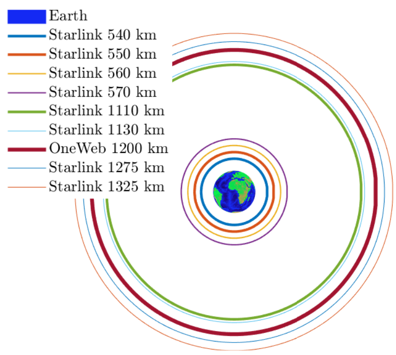

Figure 1. Schematic of the proposed mega-constellations. Thicker lines correspond to orbits with larger satellite populations.

2.1. OneWeb

The OneWeb satellite constellation (formerly WorldVu Satellites Ltd) initially intended to place a total number of 720 satellites at an altitude of 1200 km (see Figure 2). By 2020, instead, the company submitted a proposal to increase the number of satellites to 47844 satellites, to be implemented in two phases [21]. The parameters of both proposals are shown in Table 1.

Table 1. OneWeb constellation parameters

Constellation	Altitude [km]	Inclination [deg]	Planes	Number S/C	Total S/C
OneWeb Gen1	1200	87.9	18	40	720
OneWeb Gen2	1200	87.9	36	49	47844
		40	32	720	
		55	32	720	

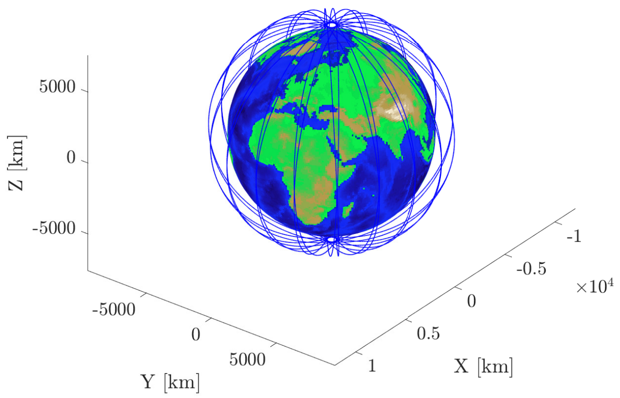

Figure 2. Schematic of the first generation of the OneWeb constellation.

According to [10], the lifetime of the constellation has been divided into 4 phases (see Figure 3). Some of them modified with the current information that can be obtained through the two-line elements (TLEs) of the currently operational spacecraft:

1. Release at 500 km and 4 months ascent to final altitude of 1200 km at 87.9° inclination.
2. Nominal orbit: 5 years of active mission at 1200 km.
3. Active disposal: 2 years using electric propulsion.
4. Passive re-entering object

Finally, the dimensions of the OneWeb constellation satellites are shown in Table 2. The main parameters are taken from [9, 10]. The average cross-sectional area has been found using CROC from ESA's DRAMA 3.0 tool suite selecting the randomly tumbling satellite option.

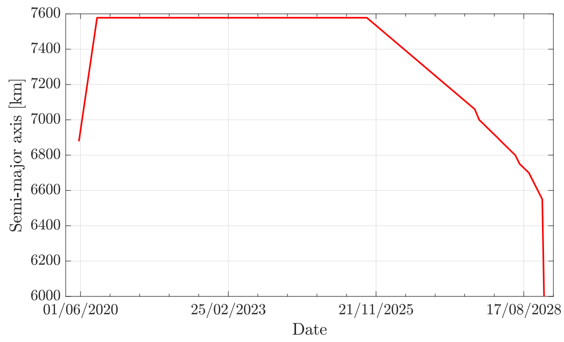

Figure 3. Evolution of the semi-major axis of the OneWeb constellation used for flux analysis.

Table 2. OneWeb satellite parameters.

Satellite Body	
Length [m]	1.0
Width [m]	1.0
Height [m]	1.0
Solar Arrays	
Length [m]	1.12
Width [m]	1.0
Overall	
Mass [kg]	147
Average cross-sectional area [m^2]	2.7
Equivalent radius [m]	0.93

2.2. Starlink

Starlink is a mega-constellation to provide broadband and global internet coverage built by SpaceX. Initially, the constellation intended to deploy 4409 satellites at different altitudes (550, 1110, 1130, 1275 and 1325 km) within the LEO regime (see Figure 4). However, in April 2020, the company modified its proposal, reducing the altitudes above 1000 km to altitudes between 540 and 570 km, changing other parameters as well as shown in Table 3.

To date, more than 1,085 satellites have been launched, of which 1,021 are still in orbit. Each launch deploys 60 satellites. In recent months, the number of launches per month has been increasing.

Analogous to the previous case, the lifetime of the constellation is divided into different phases. For those cases of the first generation of Starlink with higher altitude orbits (>1000 km), the different stages will be similar to those proposed for the case of OneWeb. Since the mass, geometry and propulsion of the satellites are different, both the ascent phase and the disposal phase have been analysed and modified. For the former, the propagation has been performed using the General Mission Analysis Tool (GMAT) assuming a total thrust of 18 mN for

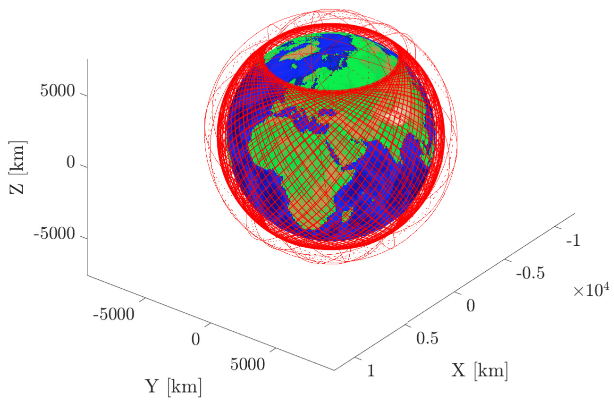

Figure 4. Schematic of the initial first generation of the Starlink constellation.

Table 3. Starlink first generation constellation parameters

Constellation	Altitude [km]	Inclination [deg]	Planes	Number S/C	Total S/C
Starlink Gen1	550	53	72	22	4409
	1110	53.8	32	50	
	1130	74	8	50	
	1275	81	5	75	
	1325	70	6	75	
Starlink Gen1 Modified	550	53	72	22	4408
	540	53.2	72	22	
	570	70	36	20	
	560	97.6	6 4	58 43	

a Krypton electric propulsion system [22]. For the disposal phase, the evaluation has been performed using the Orbital Spacecraft Active Removal tool from DRAMA suite.

For orbits between 540 km and 570 km the number of phases is reduced to three, although for the ascent and disposal phases, variations can be found based on the current data obtained through the TLEs.

1. Release at 298 km. The ascent to nominal orbit altitude can be accomplished in two ways:
    (a) Direct, from 298 km up to 550km, over a period of approximately 3 weeks.
    (b) A first ascent to 387 km of roughly 3 weeks, staying between one and two months, and a second ascent to 550 km of approximately 3 weeks.
2. Nominal orbit: 5 years of active mission at 550 km.
3. Disposal phase that can be carried out in two ways:
    (a) Passive, re-entry.
    (b) Forced active re-entry. This type of re-entry has been obtained from satellites such as Starlink-1105, on which two re-entry manoeuvres were performed: the first one descending to 450 km in a period of approximately 2 weeks and the second one descending to full re-entry in a period of approximately 1 month.

The different orbital profiles for this type of orbits are shown in Figure 5.

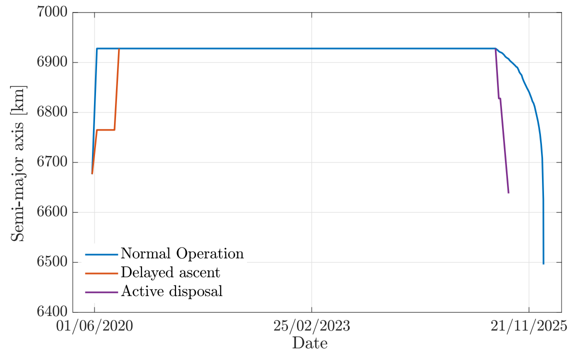

Figure 5. Evolution of the semi-major axis of the Starlink constellation used for flux analysis.

Finally, similarly to the previous case, it is necessary to define the geometrical parameters of the satellites and to obtain the average cross-sectional area of the spacecraft by means of CROC. The dimensions shown are based on Falcon 9 payload dimension data [23], taking into account that each launch deploys 60 satellites. Moreover, additional guesses such as spacers or fairing have been assumed in an attempt to obtain more conservative data.

Table 4. Starlink satellite parameters.

Satellite Body	
Length [m]	3.2
Width [m]	1.6
Height [m]	0.2
Solar Array	
Length [m]	9.6
Width [m]	3.2
Overall	
Mass [kg]	260
Average cross-sectional area [m^2]	17.5
Equivalent radius [m]	2.36

3. METHODOLOGY

The methods and formulation applied in this paper are the same as those formulated in the work of Radtke et al. [10], where the mean number of collisions N and the collision probability P are expressed as a function of the flux, the time-frame and the cross-sectional area of the satellite. First, the size of the impactors that can generate a catastrophic collision will be analysed for each of the constellations, based on the Energy-to-mass ratio (EMR). Subsequently, the flux will be calculated using MASTER. One of the main differences of this paper with respect to [10, 9] is that the new version of MASTER, MASTER-8, is used, so the object models are updated [24] with respect to the previous MASTER-2009 model [25]. In addition, MASTER-8 allows the possibility of introducing constellation traffic. Thanks to this, it will be possible to analyse the influence of the constellation itself on the flux for the whole lifetime of the mega-constellation. Additionally, a variable spacecraft lethality rate will be taken into account for both mega-constellations between 2.5% and 5.0%.

3.1. Energy-to-mass Ratio (EMR)

By calculating the Energy-to-mass ratio (EMR), it is possible to estimate the critical diameter of the space debris at which a catastrophic collision can occur for each of the satellites of the two constellations. A catastrophic collision is one in which the satellite is totally destroyed or shattered. According to [26], a catastrophic collision will occur if the threshold of 40000 J/kg is exceeded. The EMR is defined as follows:

$$EMR = \frac{M_{imp} \cdot v_{rel}^2}{2 \cdot M_{tar}} \quad (1)$$

where M_{imp} is the mass of the impactor, v_{rel} is the relative velocity at the time of the collision and M_{tar} is the mass of the target satellite. As shown in Tables 2 and 4 the mass of the target satellites will be 147 kg and 260 kg respectively. The relative velocity at the moment of impact could be as high around 14.5 km/s. Figure 6 shows the EMR evolution for both satellites and diameter evolution as a function of the mass of the impactor.

As expected, since the mass of OneWeb satellite is smaller than the Starlink mass, the mass of the impactor able to produce a catastrophic collision will be lower. Taking into account that most space debris is composed of aluminium whose density is 2.8 g/cm^3 [27], the approximate diameter to cause a catastrophic collision, assuming spherical objects, will be 3 cm and 5 cm respectively.

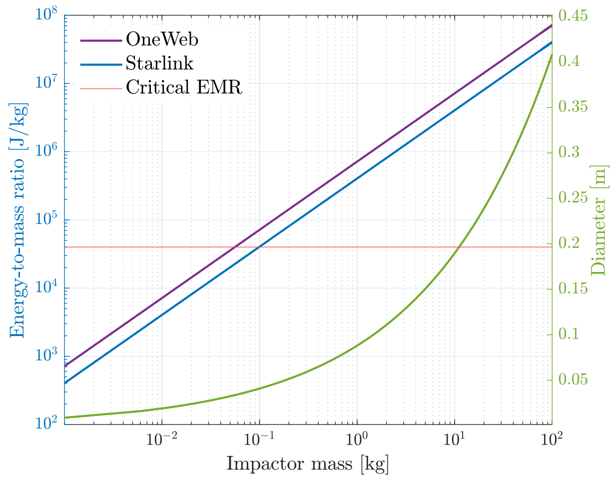

Figure 6. Energy-to-mass ratio (EMR) and impactor diameter as a function of impactor mass. Green solid line represents the diameter of the impactor as a function of its mass (assuming sphere shape and constant density). The blue and purple straight lines correspond to the evolution of EMR with respect to impactor mass. The red line corresponds to the critical EMR for a catastrophic collision to occur.

3.2. Mean number of collisions and collision probability

The diameters of the space debris will serve as input for MASTER8 to calculate the flux. Once the flux through MASTER8 has been obtained, the mean number of collisions can be calculated by:

$$N = F \cdot A_c \cdot T \quad (2)$$

where F is the flux provided by MASTER8 (according to [19], the flux is determined by the motion of the object through a stationary medium of uniform particle density at constant speed), T is the time-frame, A_c is the collision cross-sectional area calculated by means of the sum of the impactor and target (average cross-sectional area obtained through the CROC from DRAMA 3.0 suite tool) satellite radii:

$$A_c = \pi(r_{imp} + r_{tar})^2 \quad (3)$$

Equation 2 can be modified to obtain the mean number of collisions for all the objects having the same altitude and inclination in the selected constellation:

$$N_\alpha = F \cdot A_c \cdot T \cdot \alpha \quad (4)$$

being α the number of spacecraft for the selected constellation.

Once the mean number of collisions is obtained, the probability of collision will be calculated using Poisson statistics:

$$P_{i=n} = \frac{N^n}{n!} \cdot e^{-N} \quad (5)$$

where n is the number of impacts.

Thus, the probability of one or more impacts will be:

$$P_{i\geq 1} = 1 - e^{-N} \tag{6}$$

Therefore, the probability of a collision occurring in a constellation with α number of satellites having the same altitude and inclination will be:

$$P_{i\geq \alpha} = 1 - e^{-N_\alpha} \tag{7}$$

4. RESULTS

In this section the results obtained in the analysis are presented and discussed. The results obtained have been divided into two sections. Section 4.1 shows the data obtained for the flux (through MASTER8), the mean number of collisions and the collision probability for the different phases of the lifetime of each constellation. This analysis includes the effects of the constellation itself on the collision probability, as well as the increase of the spacecraft lethality rate. Then, Section 4.2 exposes the consequences of a possible collision in the constellation in terms of the analysis of the generated fragment clouds. The data has been generated using the Fragmentation Event Model and Assessment Tool (FREMAT) [28].

4.1. Flux, Mean number of collisions and collision probability

This part covers the results obtained for the flux, the mean number of collision and the collision probability. The results shown correspond to the most representative cases. For orbits at altitudes around 550 km, the Starlink case has been selected for three reasons: it is an active project, it is the only orbit that does not undergo modification, and it has a large number of satellites. For orbits above 1000 km, the cases of OneWeb at 1200 km and Starlink at 1110 km have been analysed.

The flux data have been obtained using MASTER8, therefore it should be noted:

- MASTER8 offers different types of resolution. For these cases, the most accurate one, i.e., 1 month, has been selected.
- Within the range of values for the size of the objects, the lower threshold will correspond to 3 cm for the OneWeb case and 5 cm for the Starlink cases, in accordance with the previously obtained data.
- The analyses have been performed considering both constellation and non-constellation traffic.

4.1.1. Orbits with an altitude of around 550 km

As aforementioned, the representative case of such orbits is Starlink at 550 km altitude. For the rest of the cases collected, the analysis and discussion of results can be applied in the same way taking into account that the number of satellite, the difference in altitude and the inclination may slightly affect the results shown here.

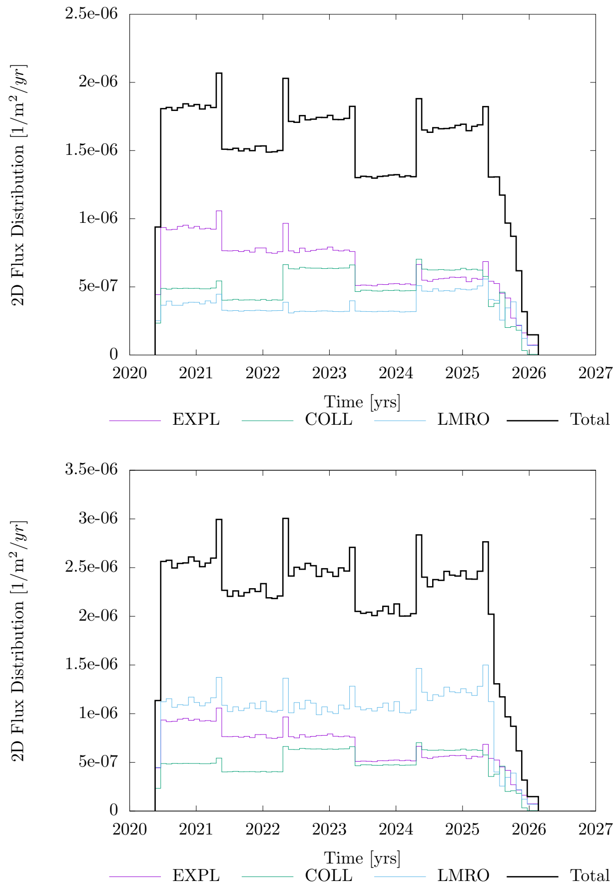

Figure 7. 2D Flux Distribution evolution over time for complete lifetime of Starlink constellation for non-constellation (up) and constellation traffic (down) at 550 km. Lower threshold diameter, $d \geq 5$ cm. Spacecraft lethality rate for constellation traffic of 5%

Figure 7 depicts the evolution of the flux for the complete lifetime of a satellite in the constellation (approximately 5.2 years). In the upper Figure the flux can be seen without the effects of constellations additional to those in the MASTER 8 catalogue. Also, the image shows that the largest values of the flux (around 1.7E-06 $1/m^2/year$) occur in the nominal orbit, and is mainly due to the effect of explosions (EXPL) and collisions (COLL). In the disposal phase, it can be seen that apart from the two previous influences, the Launch and Mission Related Objects (LMRO) also play a role.

The lower image of this same figure shows the same evolution of the flux, but adding the effects of external constellations to the MASTER8 catalogue (with a failure rate of 5%). In this case, it has been found that the constellation that most affects the flux is the satellite's own constellation, i.e., the one corresponding to an altitude of 550 km. As can be seen, once the effects of constellation traffic are introduced, the flux is increased and the main contribution is that of the LMROs, since it is in this group where the added constellations have their effect.

For this particular case, the full analysis can be found in Table 5. This analysis takes into account the different stages, as described in Section 2. Furthermore, it shows the influence of constellation traffic for different failure rates: 2.5% and 5%. The following conclusions can be drawn from the data shown:

- In the case of delayed ascent the probability of collision increases significantly compared to the normal case. This is mainly due to the longer duration, which affects the mean number of collisions.
- The collision probability is higher for the nominal operating period of the satellite, reaching almost 20% for objects of this orbital geometry. This makes sense, since the operational period constitutes almost the whole of the satellite's operational period.
- In the case of the disposal phase, similarly, the collision probability for active re-entries will be lower as the re-entry time is reduced.
- Constellation traffic increases the collision probability for all satellites in the constellation by almost 10% for the entire lifetime. This difference is even more noticeable for the nominal operating period where this probability increases by more than 45%.
- The decrease of the failure rate shows a slight decrease of the collision probability for all stages.

4.1.2. Orbits with an altitude higher than 1000 km

In this part the analysis focuses on the flux of orbits with altitudes above 1000 km.

As in the previous section, Figure 8 shows the evolution of the flux as a function of time. The lower image shows the effect of the constellation on the flux, with a failure rate of 5%. As aforementioned, the constellation effect is observed in the influence of the LMROs. Similarly, the highest flux peaks correspond to the operational period of the satellite. It is important to note that in these cases, given that the removal phase requires more time, the mean number of collision will be affected by this, and hence the collision probability for the constellation.

Table 6 shows a summary of the flux, the mean number of collisions and the collision probability for the timespan shown in the figure above. In this case, the effect of the constellation traffic on the collision probability is smaller than before, increasing it by about 5% for the total number of objects in the constellation. This may be explained by the fact that, since the re-entry time is longer, and the effect of constellation traffic does not seem to vary much at that stage, the overall increase is reduced.

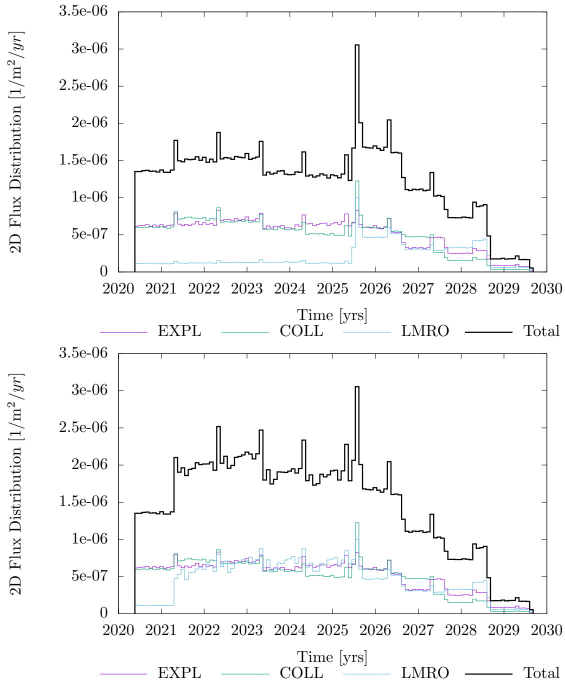

Figure 8. 2D Flux Distribution evolution over time for complete lifetime of Starlink constellation for non-constellation (up) and constellation traffic (down) at 1110 km. Lower threshold diameter, $d \geq 5$ cm. Spacecraft lethality rate for constellation traffic of 5%

The last case corresponds to the OneWeb constellation at 1200 km. It should be remembered that for this case the lower threshold for the diameter is 3 cm. Moreover, since the influence of the failure rate for the previous case has not been noticeable, only a failure rate of 5% will be taken into account. However, since the second generation of OneWeb intends to deploy almost 48000 satellites, therefore, the effects of both generations will be analysed.

For the latter case, the time evolution of its flux is shown in Figure 9 for three different cases: no-constellation traffic, constellation traffic from first generation, and constellation traffic from both generations. It is important to see that, for a similar altitude to the previous case, the average flux obtained is lower. This may be due among other things to the size of the satellite. Looking at Table 7, the first generation of satellites, 720, will increase the average flux, and therefore, the collision probability by 1%.

The most representative picture of how the number of satellites in the mega-constellation itself can increase the flux is shown below. This increase is due to the fact that the second generation of OneWeb intends to deploy around 48,000 satellites. This would increase the probability of collision risk by up to 20%, i.e., 15% more than the first generation increase.

Table 5. Flux, mean number of collisions and collision probability for Starlink at 550 km.

	Phase	F $[1/m^2/year]$	N	$P_{i\geq1}$ **(%)**	N_{1584}	$P_{i\geq1584}$ **(%)**
No Constellation Traffic	Normal ascent	5.8270E-07	5.8669E-07	0.0001	9.2932E-04	0.093
	Delayed ascent	3.8430E-07	1.8794E-06	0.0002	2.9769E-03	0.297
	Nominal operation	1.5980E-06	1.3983E-04	0.0140	2.2148E-01	19.867
	Passive re-entry	7.2290E-07	7.5211E-06	0.0008	1.1913E-02	1.184
	Active re-entry	5.5400E-07	1.5937E-06	0.0002	2.5244E-03	0.252
	Complete Lifetime	**1.5250E-06**	**1.3878E-04**	**0.0139**	**2.1982E-01**	**19.734**
Constellation Traffic Failure Rate (5%)	Normal ascent	6.5830E-07	6.6281E-07	0.0001	1.0499E-03	0.105
	Delayed ascent	4.3860E-07	2.1449E-06	0.0002	3.3976E-03	0.339
	Nominal operation	7.7200E-06	6.7550E-04	0.0675	1.0700E+00	65.699
	Passive re-entry	7.4970E-07	7.8000E-06	0.0008	1.2355E-02	1.228
	Active re-entry	6.2170E-07	1.78845E-06	0.0002	2.8329E-03	0.283
	Complete Lifetime	**2.1950E-06**	**1.9975E-04**	**0.0200**	**3.1640E-01**	**27.123**
Constellation Traffic Failure Rate (2.5%)	Normal ascent	6.5830E-07	6.6281E-07	0.0001	1.0499E-03	0.105
	Delayed ascent	4.3860E-07	2.1449E-06	0.0002	3.3976E-03	0.339
	Nominal operation	7.7160E-06	6.7515E-04	0.0675	1.0694E+00	65.680
	Passive re-entry	7.4970E-07	7.8000E-06	0.0008	1.2355E-02	1.228
	Active re-entry	6.2170E-07	1.7885E-06	0.0002	2.8329E-03	0.283
	Complete Lifetime	**2.1840E-06**	**1.9874E-04**	**0.0199**	**3.1481E-01**	**27.007**

Table 6. Flux, mean number of collisions and collision probability for Starlink at 1110 km.

	F $[1/m^2/a]$	N	$P_{i\geq1}$ (%)	N_{1600}	$P_{i\geq1600}$ (%)
No constellation traffic	1.23E-06	1.94E-04	0.019	0.31	26.67
Constellation traffic Failure rate 2.5%	1.48E-06	2.32E-04	0.023	0.3717	31.04
Constellation traffic Failure rate 5%	1.48E-06	2.32E-04	0.023	0.3719	31.06

Table 7. Flux, mean number of collisions and collision probability for OneWeb at 1200 km.

	F $[1/m^2/a]$	N	$P_{i\geq1}$ (%)	N_{720}	$P_{i\geq720}$ (%)
No constellation traffic	2.226E-6	5.108E-5	0.0051	0.0188	3.61
Constellation traffic OneWeb Gen1 Failure Rate 5%	2.533E-6	5.813E-5	0.0058	0.0418	4.10
Constellation traffic OneWeb Gen1 + Gen 2 Failure Rate 5%	1.314E-5	3.015E-4	0.030	0.217	19.52

4.2. Collision clouds

Hereafter, the results gathered from the fragment clouds obtained through the Fragmentation Event Model and Assessment Tool (FREMAT) are shown. This tool implements the industry-standard NASA fragmentation model (through the Fragmentation Event Generator, FREG) to subsequently propagate the fragmentation events (Impact of Fragmentation Events on Spatial Density Tool, IFEST) using a semi-analytical propagation (refer to [28] for more information).

The analysis was conducted from two perspectives. On the one hand, the catastrophic collision is produced by an exogenous object to the constellation (e.g., space debris). On the other hand, since the satellites of mega-constellations have a failure rate, it is possible that two of these satellites lose their manoeuvrability, become uncontrollable and may collide with each other, i.e., an endogenous collision. Furthermore, given the configurations for both mega-constellations, these collisions have been simulated for two different altitudes: one simulation for those orbital planes located around 550 km altitude and the other for altitudes above 1000 km. In the latter case, a simulation has been generated for both mega-constellations. For all simulations the intersection of both colliding objects occurs in orbits rotated 90 degrees with respect to their RAAN.

4.2.1. Collisions at altitudes around 550 km

First, the results obtained by the collision of an exogenous object with one of the Starlink satellites at an altitude of 550 km are analysed. Figure 10 shows the fragment cloud generated one day after the impact. Hundreds of fragments were generated after the collision with sizes between 1 and 10 cm.

Figure 11 shows the Gabbard plots for the satellite that has experienced the collision for two dates: the day immediately after the collision and three years later. As expected, most of the fragments have re-entered within three years. This same conclusion can be seen in Figure 12 where it can be observed the evolution of the spatial

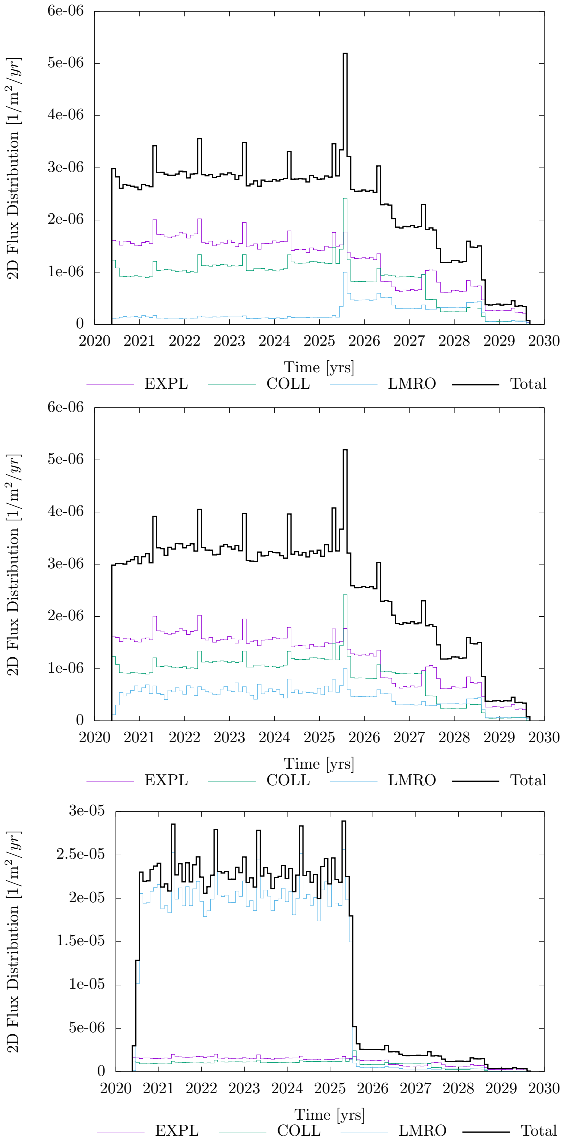

Figure 9. 2D Flux Distribution evolution over time for complete lifetime of OneWeb constellation for non-constellation (up), Gen1 constellation traffic (middle) and Gen1+Gen2 constellation traffic (down) at 1200 km. Lower threshold diameter, $d \geq 3$ cm. Spacecraft lethality rate for constellation traffic of 5%

density created by the fragments generated in the collision which is drastically reduced in a period of approximately one year.

The collision between two satellites of the same constellation with a mass of 260 kg is then simulated. From Figure 13 it can be observed how the clouds of fragments generated are more numerous than for the exogenous case, spawning thousands of fragments (around 15000) in each of the objects in a similar size range to the previous case.

As in the previous case, Figure 14 shows the evolution of the spatial density of the fragment clouds generated

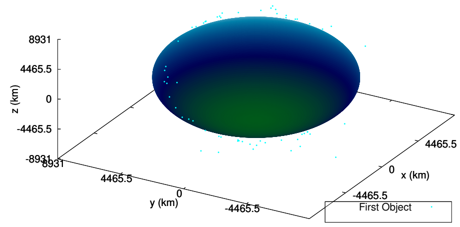

Figure 10. Cloud of fragments after 1 day. Starlink exogenous collision at 550 km

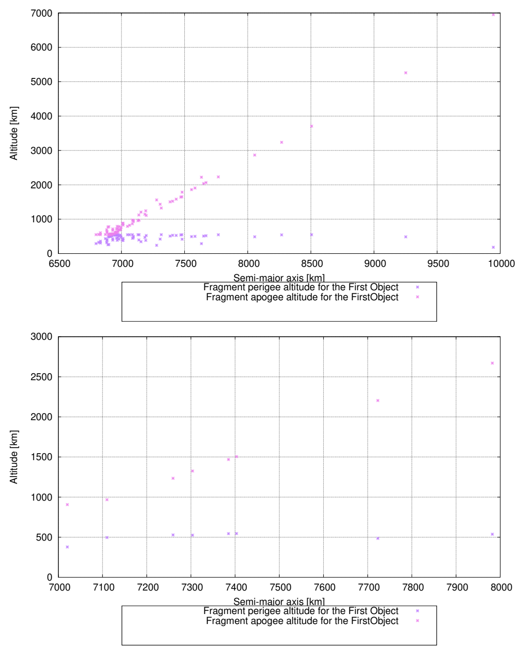

Figure 11. Gabbard diagram for the fragmentation cloud the day after the collision (up) and three years later (down). Starlink exogenous collision at 550 km

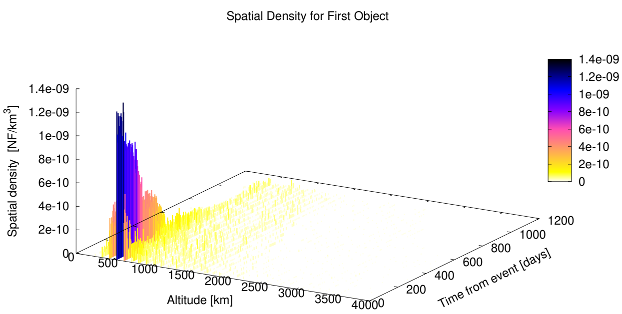

Figure 12. Spatial density over 3 years for the colliding satellite. Starlink exogenous collision at 550 km

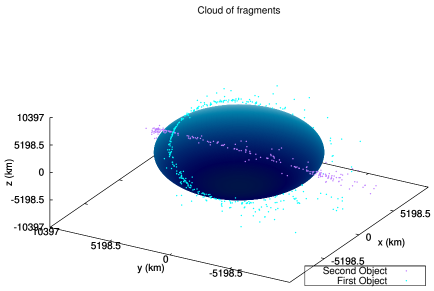

Figure 13. Cloud of fragments after 1 day. Starlink endogenous collision at 550 km

by each of the objects after the collision. Again, it can be observed that for both fragment clouds most of them re-enter in a time period of one year.

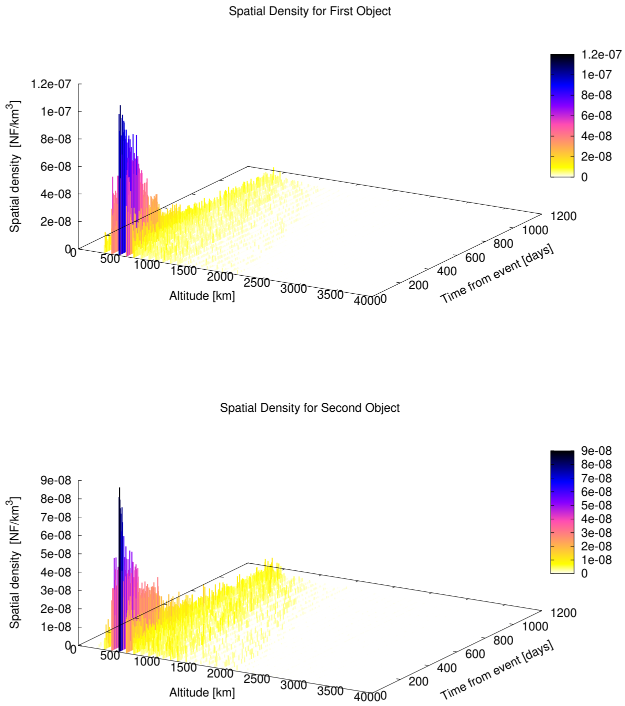

Figure 14. Spatial density over 3 years for first colliding satellite (up) and second colliding satellite (down). Starlink endogenous collision at 550 km

FREMAT also allows to analyse the percentage increase in spatial density with respect to the MASTER2009 object catalogue. Figure 15 shows this percentage increase with respect to the background objects. It can be seen that the increase is higher for the first year after the collision, since, as mentioned above, most objects re-enter after that period of time. This increase range from 40% to more than 100% for the first year.

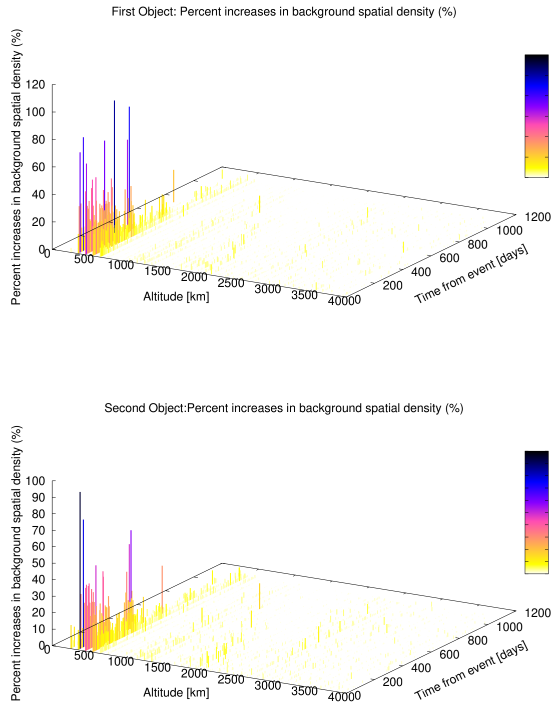

Figure 15. Percent increases in background spatial density (MASTER2009) as a function of altitude and time for the first object (up) and second object (down). Starlink endogenous collision at 550 km

4.2.2. Collisions at altitudes higher than 1000 km

Analogously to the previous case, the analysis can be performed for orbital profiles at altitudes above 1000 km. The first case analysed corresponds to the fragmentation by a catastrophic collision of a OneWeb satellite, with a mass of 147 kg and located at an altitude of 1200 km. Figure 16 shows the fragment cloud generated 1 day after the fragmentation.

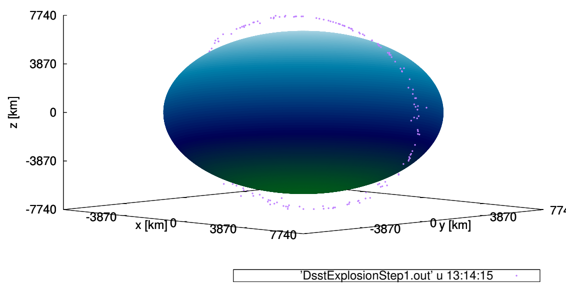

Figure 16. Cloud of fragments after 1 day. OneWeb exogenous collision at 1200 km

Figure 17 depicts the Gabbard diagrams of the fragmentation for the time after the collision and five years later (the impactor has a diameter of 3cm, which is the critical value for a catastrophic collision). In contrast to the cases with altitudes around 550 km, it can be seen that almost all fragments remain at the same apogee and perigee as immediately after the fragmentation, i.e., most of the fragments will remain in the orbital plane of the collision. These results are close to what obtained in [10] performing a similar analysis for the OneWeb constellation.

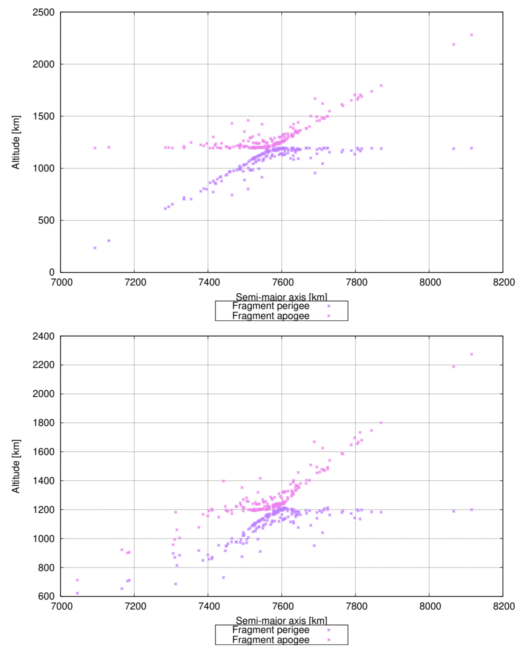

Figure 17. Gabbard diagram for the fragmentation cloud the day after the fragmentation (up) and three years later (down). OneWeb exogenous collision at 1200 km

Furthermore, Figure 18 shows the evolution of spatial density over a five-year period, consolidating that the fragments do not re-enter after a long period of time. This is a good argument in favour of constellations at low altitudes.

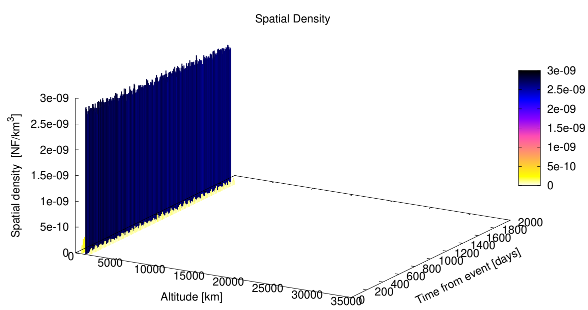

Figure 18. Spatial density over 5 years for the colliding satellite. OneWeb exogenous collision at 1200 km

Finally, the collision between two objects in the same constellation has also been simulated for orbits at these altitudes. For this case, the Starlink constellation at 1110 km altitude has been chosen. Again, the mass of the satellites is 260 km. Figure 19 shows the fragment cloud after the collision.

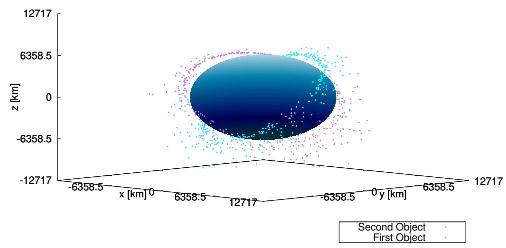

Figure 19. Cloud of fragments after 1 day. Starlink endogenous collision at 1110 km

Figure 20 represents the evolution of the spatial density of the two fragment clouds generated by the collision over a period of 5 years. As in the case of the exogenous collision, it can be seen that there is hardly any variation with respect to time in the spatial density, indicating that most of the fragments will remain in these orbital planes, at least for the entire operational lifetime of the constellation satellites.

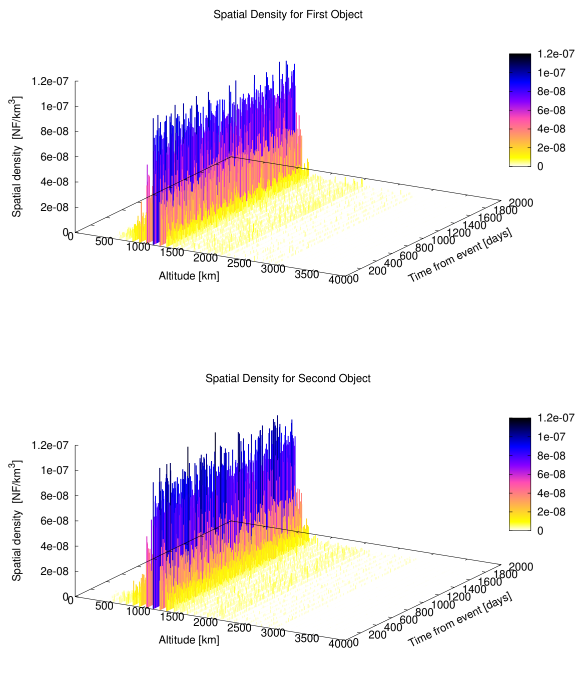

Figure 20. Spatial density over 5 years for first colliding satellite (up) and second colliding satellite (down). Starlink endogenous collision at 1110 km

To conclude the section, the percentage increase in spatial density with respect to the background density provided by MASTER2009 is shown. In this case, the increase in spatial density also remains constant over time. The increases for the collision altitude are between 60% and 120%. It is interesting to note that there is also a slight increase of the spatial density in higher orbits, mainly because these are orbits with a low occupancy level.

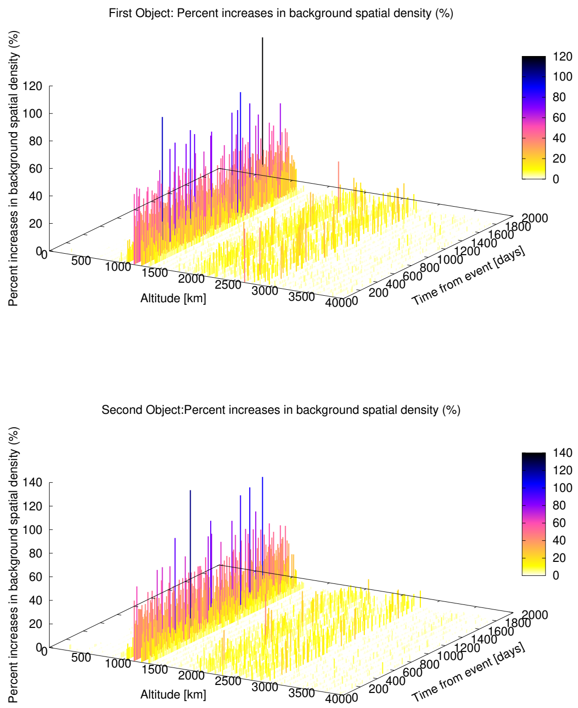

Figure 21. Percent increases in background spatial density (MASTER2009) as a function of altitude and time for the first object (up) and second object (down). Starlink endogenous collision at 1110 km

5. SUMMARY AND CONCLUSIONS

An analysis of the effects of mega-constellations on the collision risk in space has been carried out in this study. First, previous literature and analyses have been introduced to try to discern the problematic nature of the problem. Then, the main parameters of the mega-constellations used during this analysis were presented, emphasising the difficulty in finding information due to the private nature of these projects. Once the parameters of the problem have been determined, the methodology applied for the risk analysis and the probability of collision used have been explained, based mainly on defining catastrophic collisions, in order to delimit the study and thus obtain the probability of collision.

Taking into account the flux obtained in orbits between 540 km and 570 km, the risk of the constellation itself has been reflected in the probability of collision (up to 10%), being critical in the nominal operation stage of the satellite (up to 45%), as it has the longest duration. In addition, the different stages have been analysed, taking into account possible variations such as an active re-entry. For the cases with orbits higher than 1000 km, it was found that the increase in the probability of collision is mainly due to the fact that both the ascent and re-entry times are longer. In the case of Starlink, the constellation effect increases the total collision probability by about 5%. For the OneWeb case it has been concluded that the effect of adding the 48000 second generation satellites would be hazardous in terms of collision probability.

Finally, the analysis of exogenous catastrophic collisions and possible endogenous collisions was carried out. For orbits with lower altitudes, it can be concluded that even if the re-entry of fragments occurs in a short time, the increase in the number of objects produced for these orbits could be catastrophic due to a possible cascade effect. For orbits higher than 1000 km, although they are less busy orbits, the problem is not eradicated since for these cases the fragments remain almost immutable for a long period of time, or at least a period equal to the lifetime of the satellites in the constellation.

ACKNOWLEDGMENTS

The authors would like to extend their thanks to Jonas Radtke (OKAPI:Orbits) for his expertise and support provided. In addition, the authors would like to acknowledge the support of the ESA's Space Debris User Portal (SDUP), especially Vitali Braun for his assistance with MASTER issues.

REFERENCES

[1] ESA Space Debris Office. Esa's annual space environment report, 2020.

[2] Donald J Kessler and Burton G Cour-Palais. Collision frequency of artificial satellites: The creation of a debris belt. *Journal of Geophysical Research: Space Physics*, 83(A6):2637–2646, 1978.

[3] L Anselmo, A Rossi, and C Pardini. Updated results on the long-term evolution of the space debris environment. *Advances in Space Research*, 23(1):201–211, 1999.

[4] Donald J Kessler. Collisional cascading: The limits of population growth in low earth orbit. *Advances in Space research*, 11(12):63–66, 1991.

[5] J-C Liou and Nicholas L Johnson. Instability of the present leo satellite populations. *Advances in Space Research*, 41(7):1046–1053, 2008.

[6] Carmen Pardini and Luciano Anselmo. Review of past on-orbit collisions among cataloged objects and examination of the catastrophic fragmentation concept. *Acta Astronautica*, 100:30–39, 2014.

[7] A Rossi, A Cordelli, P Farinella, L Anselmo, and C Pardini. Long term evolution of the space debris population. *Advances in Space Research*, 19(2):331–340, 1997.

[8] Chuan CHEN and Wulin YANG. The impact of large constellations on space debris environment and its countermeasures, 2017.

[9] S Le May, S Gehly, BA Carter, and S Flegel. Space debris collision probability analysis for proposed global broadband constellations. *Acta Astronautica*, 151:445–455, 2018.

[10] Jonas Radtke, Christopher Kebschull, and Enrico Stoll. Interactions of the space debris environment with mega constellations—using the example of the oneweb constellation. *Acta Astronautica*, 131:55–68, 2017.

[11] B Bastida Virgili, JC Dolado, HG Lewis, J Radtke, H Krag, B Revelin, C Cazaux, CAMILLA Colombo, R Crowther, and M Metz. Risk to space sustainability from large constellations of satellites. *Acta Astronautica*, 126:154–162, 2016.

[12] Carmen Pardini and Luciano Anselmo. Environmental sustainability of large satellite constellations in low earth orbit. *Acta Astronautica*, 170:27–36, 2020.

[13] Romain Lucken and Damien Giolito. Collision risk prediction for constellation design. *Acta Astronautica*, 161:492–501, 2019.

[14] Nathan Reiland, Aaron J Rosengren, Renu Malhotra, and Claudio Bombardelli. Assessing and minimizing collisions in satellite mega-constellations. *Advances in Space Research*, 2021.

[15] B. D. Weimer. Application for fixed satellite service by worldvu satellites limited, debtor-in-possession sat-mpl-20200526-00062 / satmpl2020052600062, 2020.

[16] W. Wiltshire. Application for fixed satellite service by space exploration holdings, llc sat-mod-20200417-00037 / satmod2020041700037, 2020.

[17] W. Wiltshire. Application for fixed satellite service by space exploration holdings, llc sat-loa-20200526-00055 / satloa2020052600055, 2020.

[18] J. D. Hindin. Application for fixed satellite service by kuiper systems llc sat-loa-20190704-00057 / satloa2019070400057, 2019.

[19] Heiner Klinkrad. Space debris. *Encyclopedia of Aerospace Engineering*, 2010.

[20] V. Braun. From measurements to uncertainties to understanding. 1st esa's master workshop 2021., 2021.

[21] B. D. Weimer. Application for modification. modification to oneweb sat-mpl-2020, 2020.

[22] MICHAEL PATTERSON and GEORGE WILLIAMS, JR. Krypton ion thruster performance. In *28th Joint Propulsion Conference and Exhibit*, page 3144, 1992.

[23] SpaceX. Falcon 9 user's guide, 2020.

[24] A. Horstmann. Master-8 final report. enhancement of s/c fragmentation and environment evolution models.

[25] S Flegel, J Gelhaus, C Wiedemann, P Vorsmann, M Oswald, S Stabroth, H Klinkrad, and H Krag. The master-2009 space debris environment model. In *Fifth European Conference on Space Debris*, volume 672, pages 1–8. European Space Agency/European Space Operations Centre Darmstadt, Germany, 2009.

[26] DS McKnight. Collision and breakup models: Pedigree, regimes, and validation/verification. In *Briefing presented to the National Research Council Committee on Space Debris Workshop, Irving, California, November*, volume 18, 1993.

[27] John N Opiela. A study of the material density distribution of space debris. *Advances in Space Research*, 43(7):1058–1064, 2009.

[28] Roxana Larisa Andrișan, Alina Georgia Ioniță, Raúl Domínguez González, Noelia Sánchez Ortiz, Fernando Pina Caballero, and Holger Krag. Fragmentation event model and assessment tool (fremat) supporting on-orbit fragmentation analysis. In *7th European Conference on Space Debris*, 2017.